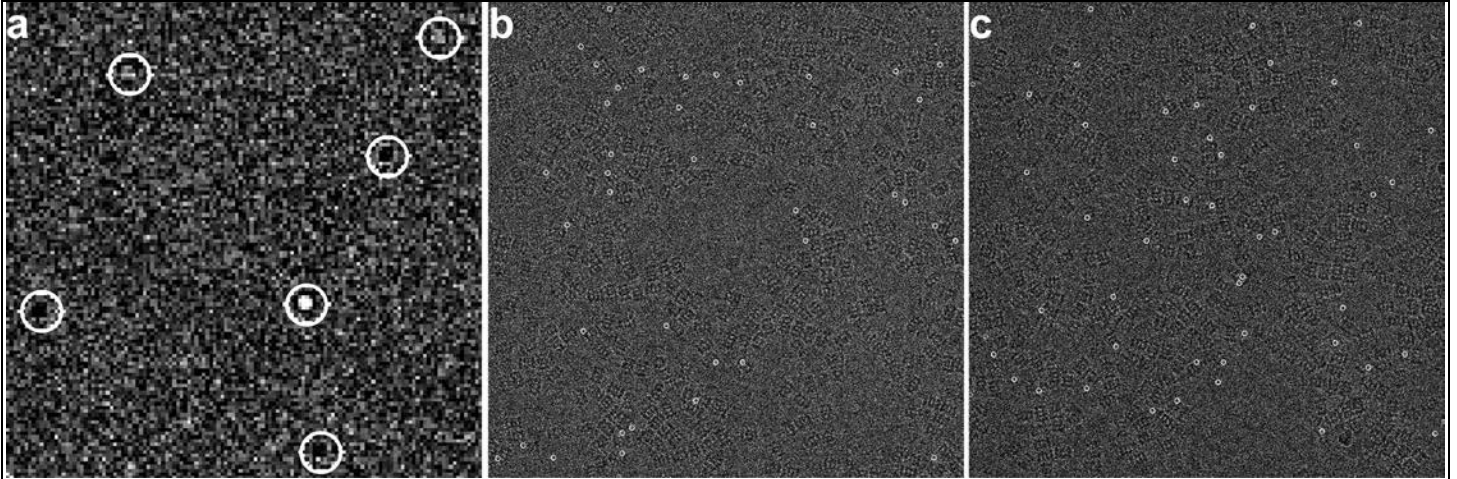


Supplementary Figure 1

A doming model describes the motion of frozen hydrated samples induced by the high-energy electron beam.

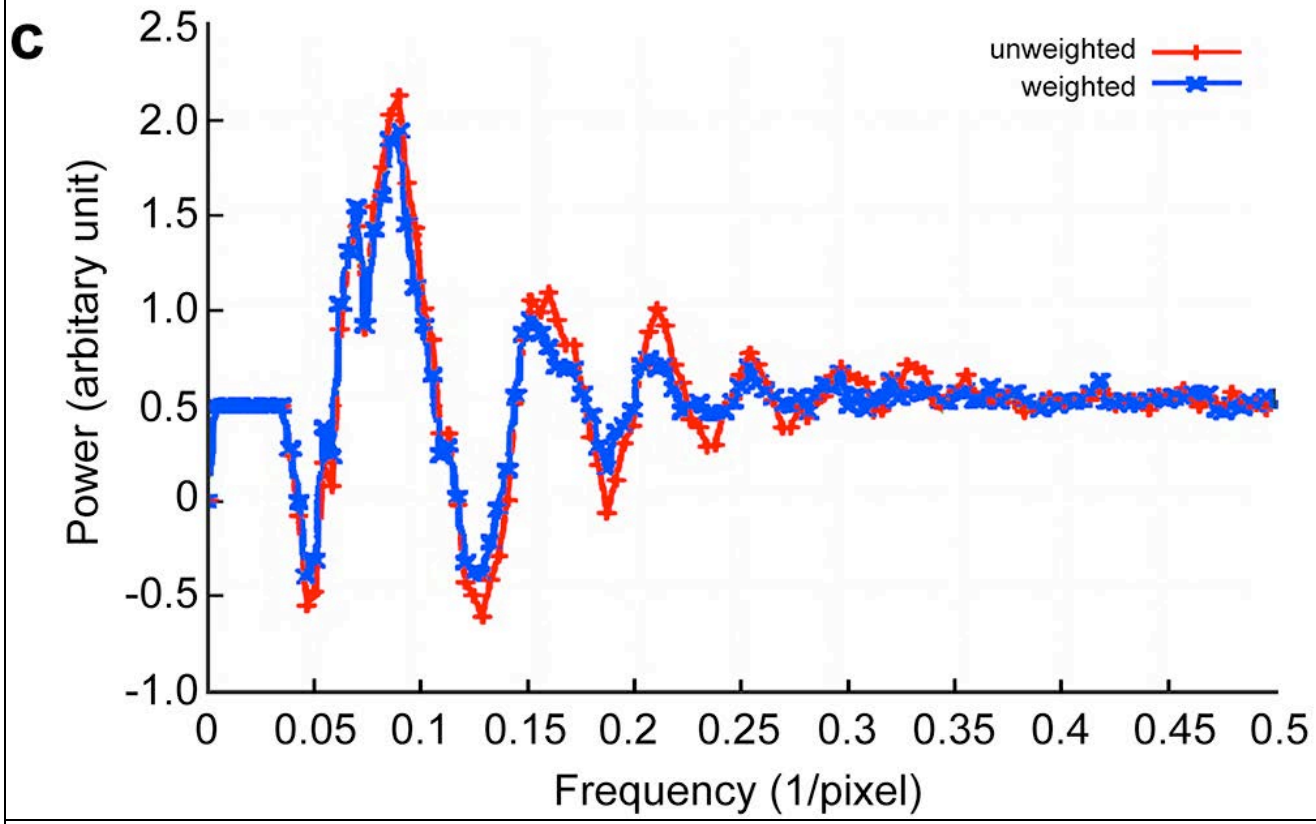
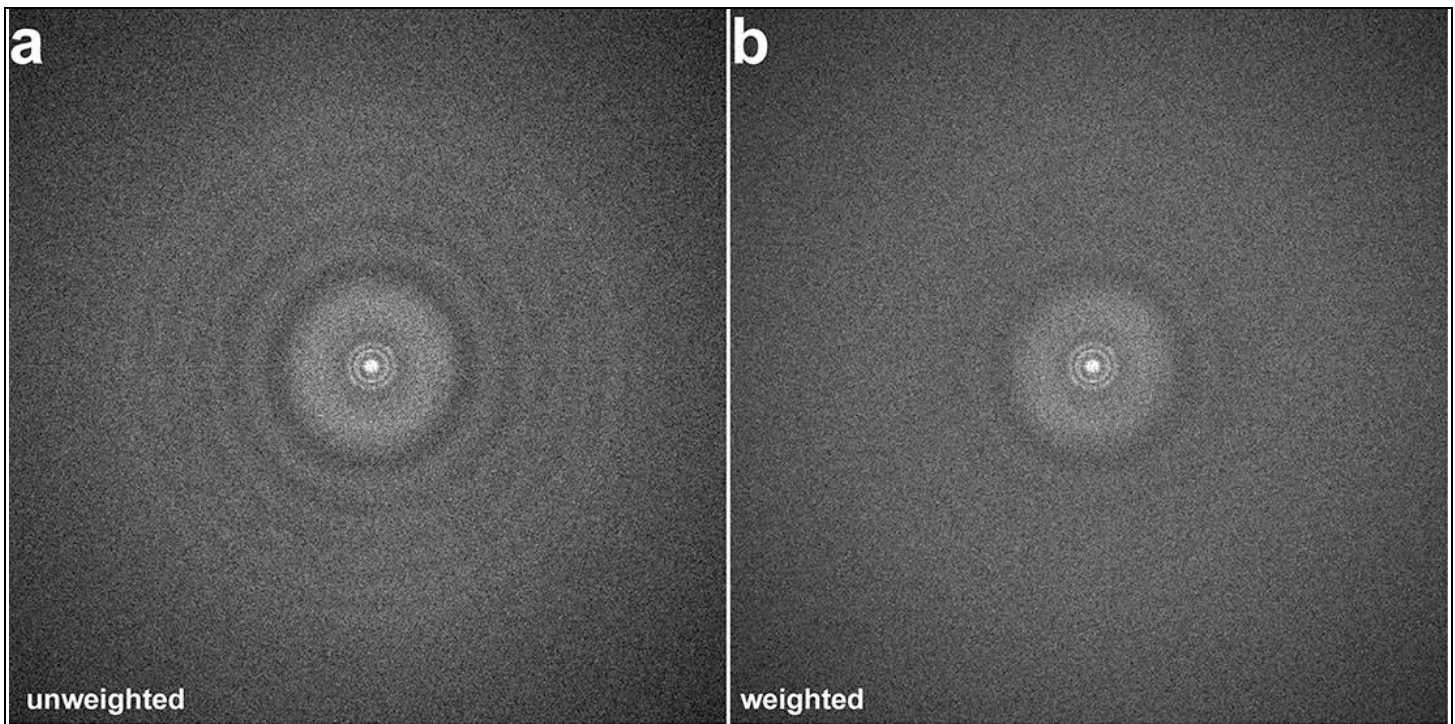
(a) Traces of the projected motion measured at three different tilt angles (α -angle) extracted from a dose fractionated tilt series acquired on a frozen hydrated specimen of a wild-type *Drosophila melanogaster* γ -Tubulin Ring Complex. The black arrow in the plot indicates the starting position of the motion. (b) Image of frozen hydrated archaeal 20S proteasome overlaid with the traces of global motion based upon whole frame alignment (long trace originated from the center of image) and each patch determined from MotionCor2. The whole frame is divided into 5×5 patches, and traces of each patch are determined individually. The traces of the global and local motions are exaggerated on the image by a factor of 145. For perspective, the accumulated global motion is ~ 11 Å.



Supplementary Figure 2

Defect pixel detection in MotionCor2

(a) An example showing defective pixels (marked with white circles) in an image captured with the K2 Summit camera. (b) and (c) Two different images collected one after the other show pixel defects (marked with white circles) in different locations.

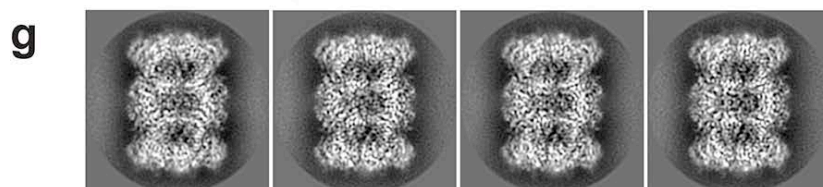
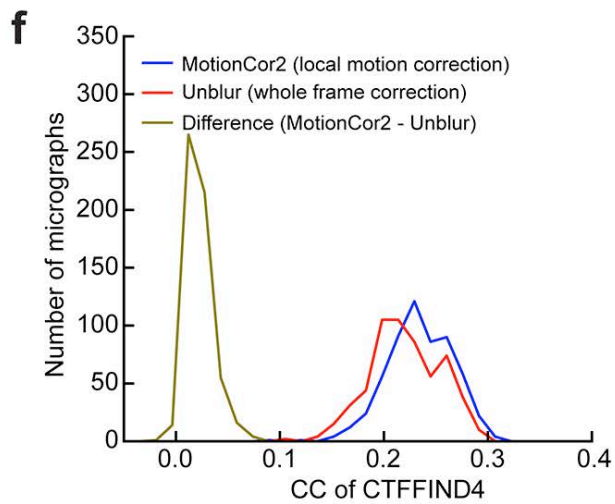
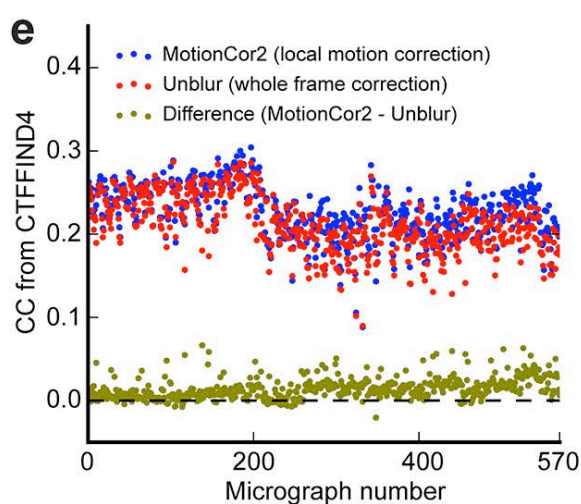
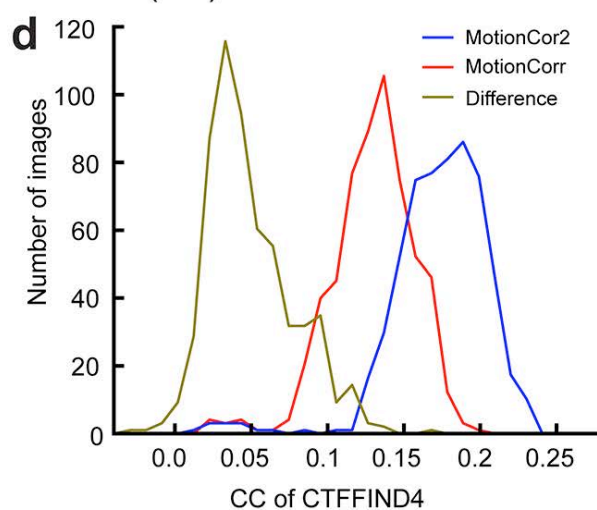
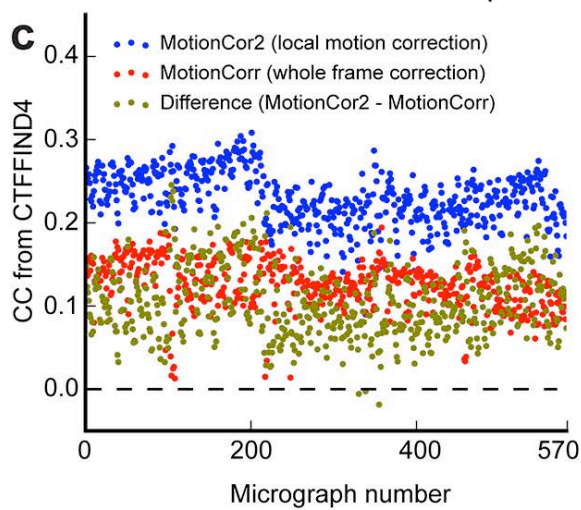
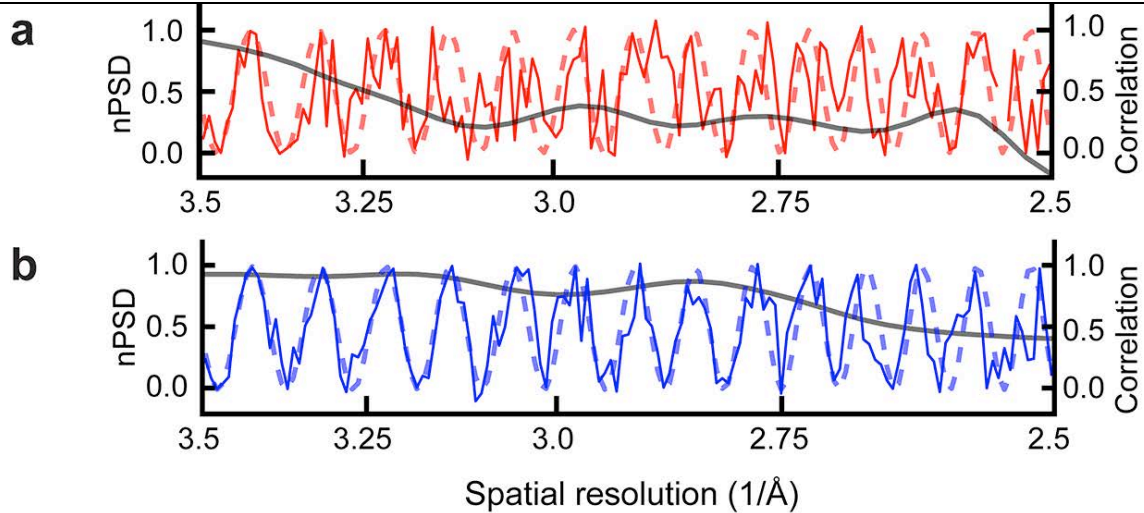


Supplementary Figure 3

Influence of dose weighting on the Fourier power spectrum

(a) and (b) Fourier power transform calculated from dose-weighted (a) and un-weighted (b) image after motion correction. (c) The rotation averages

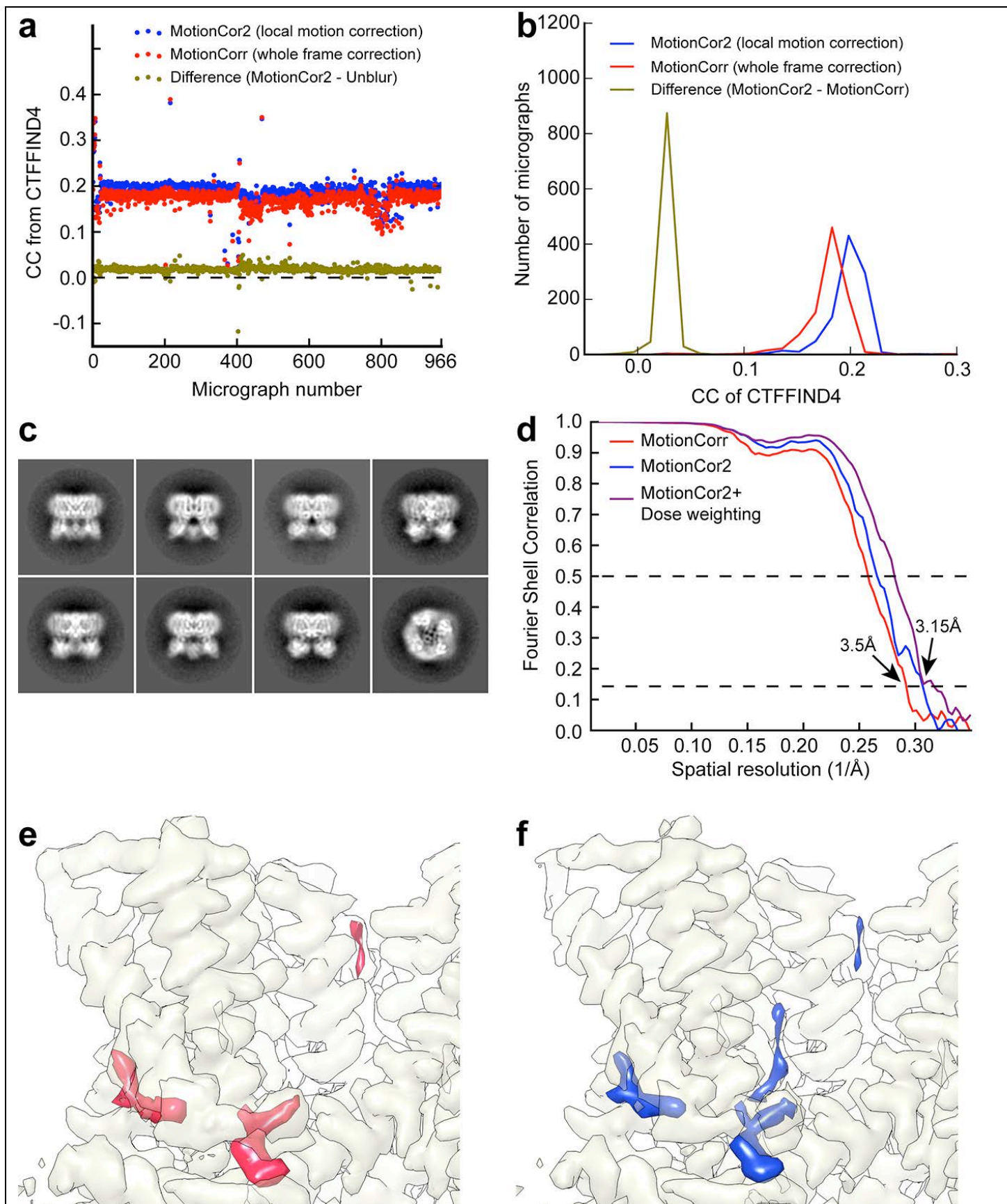
of dose-weighted (blue) and un-weighted (red) Fourier power spectra shown in (a) and (b).



Supplementary Figure 4

Comparison of motion corrections by MotionCor2 and MotionCorr on 3D reconstruction of archaeal 20S proteasome.

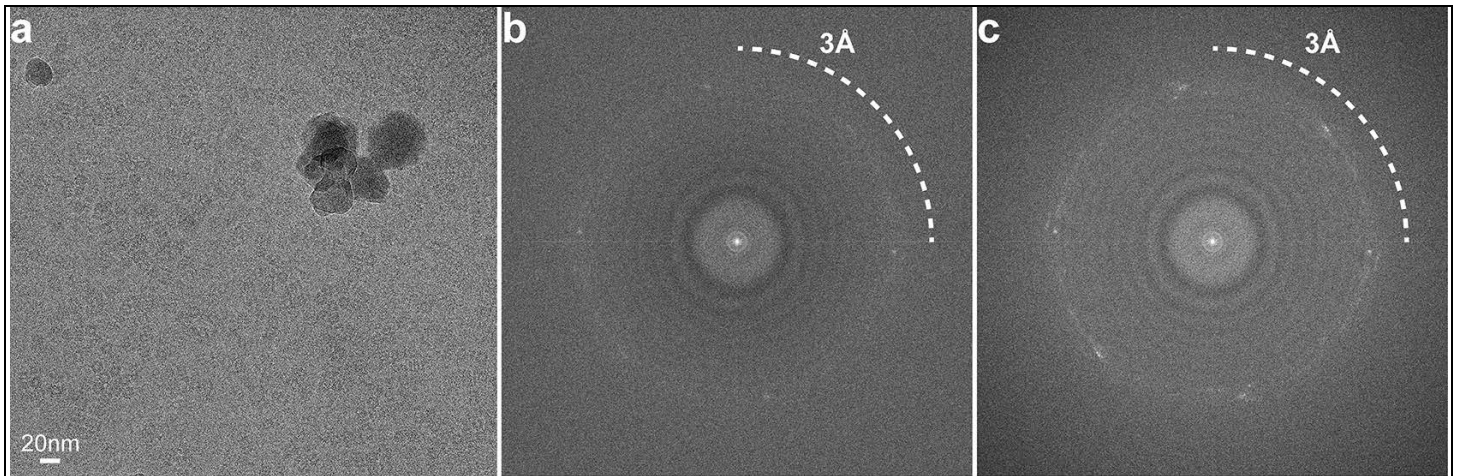
(a) Rotationally averaged Fourier power spectrum of image after motion correction by MotionCorr (solid line) and fitted contrast transfer function (dashed line). (b) Rotationally averaged Fourier power spectrum of image after motion correction by MotionCor2 (solid line) and fitted CTF (dashed line). Solid black line in both (a) and (b) indicate cross correlation coefficient between the rotationally averaged Fourier power spectrum of image and fitted CTF. (c) The cross correlation coefficient output from CTFFIND4 was used to assess the Thon ring quality within the resolution range of 10 ~ 5 Å. Blue and red dots represent cross correlation coefficient of every micrograph after motion correction using MotionCor2 (blue) and MotionCorr (red). Brown dots represent the differences between the two. (d) Histogram of cross correlation coefficients between calculated and simulated Fourier power spectrum of MotionCorr corrected image (red) and MotionCor2 corrected image (blue). The difference, which shows the amount of improvement, is shown in brown. (e) Comparison of motion corrections by MotionCor2 and Unblur. The cross correlation coefficient output from CTFFIND4 calculated within the resolution range of 10 ~ 5 Å. Blue and red dots represent cross correlation coefficient of every micrograph after motion correction using MotionCor2 (blue) and Unblur (red). Brown dots represent the differences between the two. (f) Histogram of cross correlation coefficients between calculated and simulated Fourier power spectrum of MotionCor2 corrected image (blue) and Unblur corrected image (red). The difference, which shows the amount of improvement, is shown in brown. (g) Selected 2D class averages of 20S proteasome calculated from images after motion correction by MotionCor2.



Supplementary Figure 5

Comparison of motion correction by MotionCor2 and MotionCorr on 3D reconstruction of rat TRPV1 ion channel.

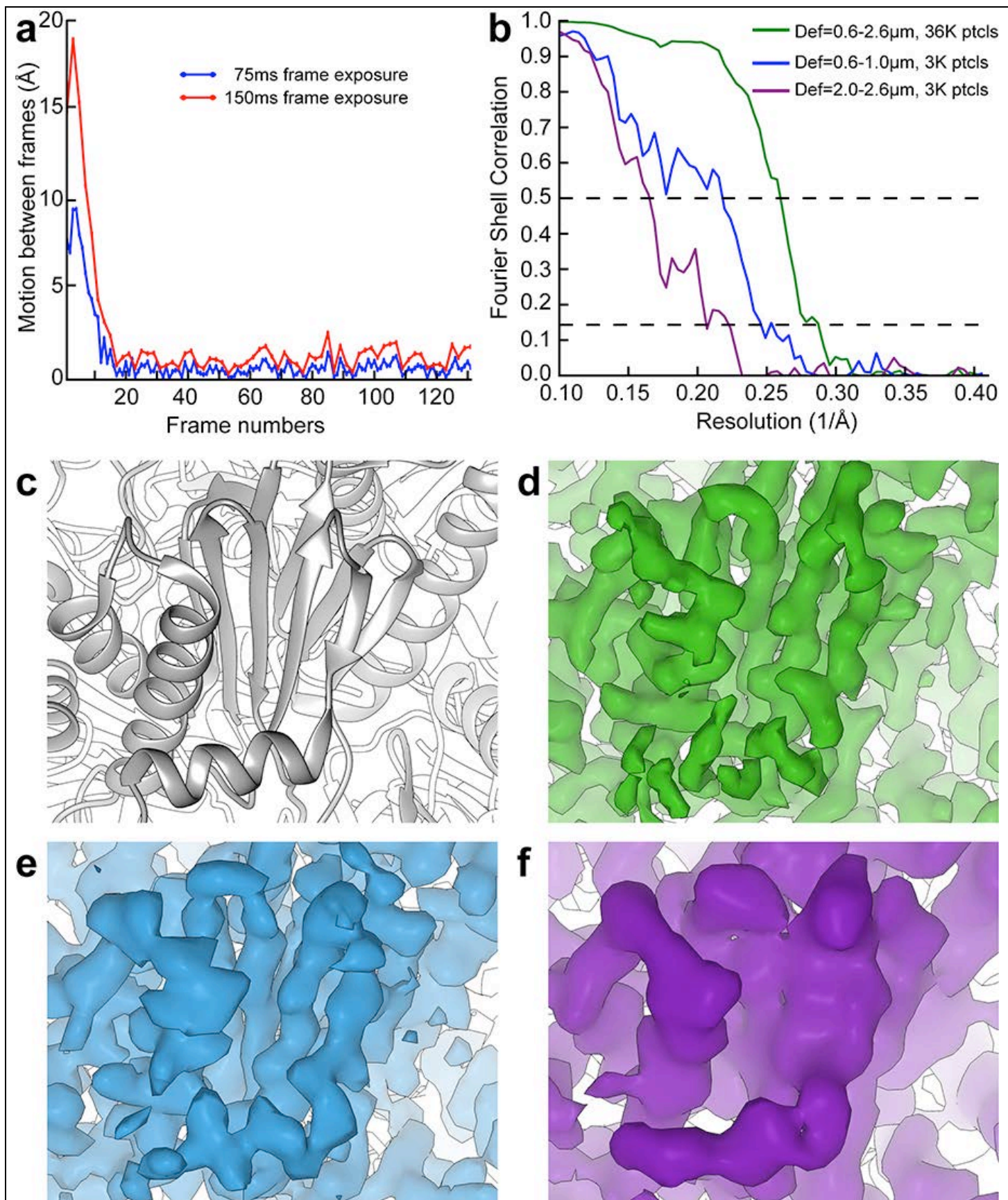
A published dataset of frozen hydrated rat TRPV1 ion channel was reprocessed using MotionCor2. (a) Cross Correlation Coefficient of CTFFIND4⁹ from the correction by both MotionCorr (red) and MotionCor2 (blue). (b) Histogram of cross correlation coefficients determined by using CTFFIND4 using image corrected by MotionCor2 (blue) and MotionCorr (red). The difference, which shows the amount of improvement, is shown in brown. (c) Representative 2D class averages of frozen hydrated TRPV1 particles. (d) FSC curves of 3D reconstructions determined from the same dataset after motion correction by MotionCorr (red), MotionCor2 (blue) and MotionCor2 with dose weighting (brown). (e) A representative view of the TRPV1 ion channel generated from previously published density map⁵. (f) The view of the same region of TRPV1 density map determined after re-process motion correction using MotionCor2. Both maps (e and f) are shown at the same normalized density level, $\sigma = 6$.



Supplementary Figure 6

Motion correction of low defocused image.

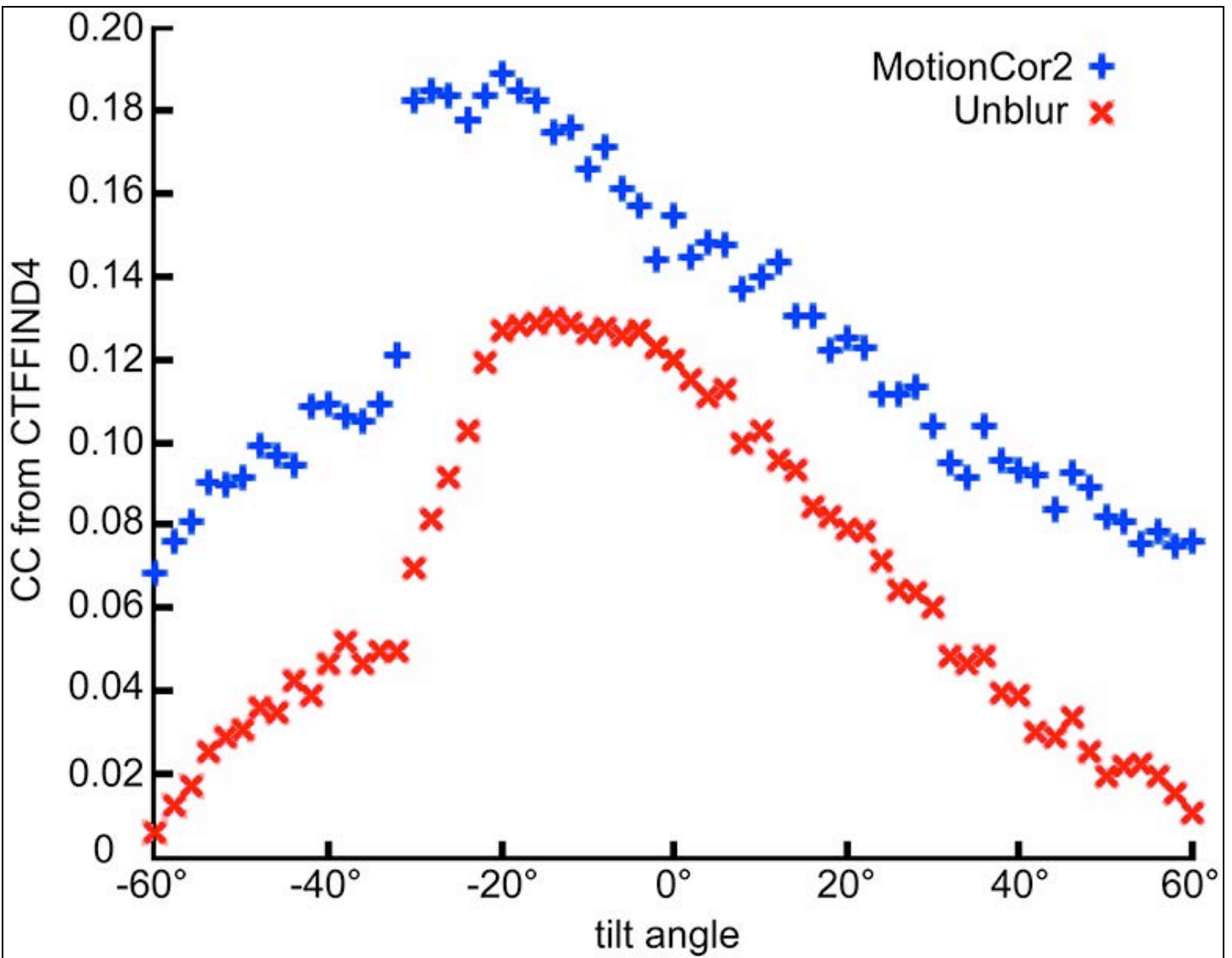
(a) A micrograph of frozen hydrated archaeal 20S proteasome recorded with a defocus of $0.4\ \mu\text{m}$ at 200kV on a TF20. (b) and (c) Fourier power spectra are shown from the same image before motion correction (b), and after motion correction with MotionCorr (c). The motion correction of the same micrograph by MotionCorr failed.



Supplementary Figure 7

3D reconstruction of archaeal 20S proteasome from a TF20 200kV electron microscope.

(a) A plot of motion between neighboring frames when frame exposure was set to 0.075 second (blue) and 0.15 second (red, by average two adjacent sub-frames to produce a sub-frame that is equivalent to the 0.15 second frame exposure time). (b) Red: FSC curve of an archaeal 20S proteasome 3D reconstruction determined from a dataset of ~36,000 particles collected with a TF20 electron microscope operated at 200kV acceleration voltage. The defocus range was set between 0.6 μ m and 2.6 μ m. Blue: FSC curve of a 3D reconstruction using a subset of 3,000 particles with low defocus (0.6 μ m to 1 μ m). Purple: FSC curve of a 3D reconstruction of using another subset of 3,000 particles high defocus (2.0 μ m to 2.6 μ m). (c) Ribbon diagram of a part of archaeal 20S proteasome. (d) Same region of the 3D reconstruction determined from the entire dataset, corresponding to red FSC curve in (a). (e) Same region of the 3D reconstruction determined from the subset of 3,000 particles with only low defocused particles (blue FSC curve). (f) Same region of the 3D reconstruction determined from a subset of 3,000 particles with only high defocused particles (purple FSC curve). All maps (d, e and f) are shown at the same normalized density level, $\sigma = 4$.



Supplementary Figure 8

Comparison of Unblur and MotionCor2 on a tomographic tilt series.

This tomographic tilt series was collected between $[-60^\circ, 60^\circ]$ at every 2° from a frozen hydrated specimen of *Drosophila* centriole. The data collection was performed in two branches that started from -30° to 60° and then from -32° to -60° and at the magnification that gives rise to the pixel size of 4.08\AA . At each angular step a movie stack of 20 sub-frames was collected at dose rate of $5e^-/\text{pixel}/s$ with frame exposure of $0.25s$. Under this setup the per-frame dose is $0.075e^-/\text{\AA}^2$ and the total dose of the entire tilt series is $92e^-/\text{\AA}^2$.